

# **A New Servo Control Drive for Electro Discharge Texturing System Industrial Applications Using Ultrasonic Technology**

M. Shafik<sup>1,\*</sup>, H. S. Abdalla<sup>2</sup>

<sup>1</sup>Faculty of Art & Design and Technology, University of Derby, UK.

<sup>2</sup>School of Architecture, Computing and Engineering, University of East London, London, UK.

Received 21 April 2013; received in revised form 20 May 2013; accepted 10 June 2013

## **Abstract**

This paper presents a new ultrasonic servo control drive for electro discharge texturing system industrial applications. The new drive is aiming to overcome the current teething issues of the existing electro discharge texturing system, servo control drive level of precision, processing stability, dynamic response and surface profile of the machined products. The new ultrasonic servo control drive consists of three main apparatuses, an ultrasonic motor, electronic driver and control unit. The ultrasonic motor consists of three main parts, the stator, rotor and sliding element. The motor design process, basic configuration, principles of motion, finite element analysis and experimental examination of the main characteristics is discussed in this paper. The electronic driver of the motor consists of two main stages which are the booster and piezoelectric amplifier. The experimental test and validation of the developed servo control drive in electro discharge texturing platform is also discussed and presented in this paper. The initial results showed that the ultrasonic servo control drive is able to provide: a bidirectional of motion, a resolution of <math>50\mu\text{m}</math> and a dynamic response of <math>10\text{msec}</math>. The electron microscopic micro examination into the textured samples showed that: a clear improvement in machining stability, products surface profile, a notable reduction in the processing time, arcing and short-circuiting teething phenomena.

**Keywords:** ultrasonic servo drive, servomotors, EDT, mechatronics

## **1. Introduction**

Level of precision, resolution, dynamic time response, robust stability of machining, miniaturisation of the parts and cost are the main design considerations of servo control systems, as these essential sceneries offer a selection of flexibility and open new possible commercial opportunities for servo drives technology industrial applications. Servo control drives using DC/AC servomotors have been known for more than hundred of years and have many applications in the areas of process and machine control.

Machining and process control can be classified according to the level of precision and dynamic time response as normal machining, precision machining, high precision machining and ultrahigh precision machining. In the mid-1940s servo control drive using DC/AC servomotor technology were implemented in Electro Discharge Machining (EDM) applications. EDM

---

\* Corresponding author. E-mail address: m.shafik@derby.ac.uk

Tel.: +44 (0) 1332593170; Fax: +44 (0) 1332622739

applications are classified as high precision machining. The main principle of operation of EDM is based mainly on a spark discharge between two conducting surfaces separated by a dielectric medium. The generated spark duration is on the order of microseconds and the inter-electrode gap size is of 10 to 100 micrometers. EDM is widely used in various applications including creating different complex and intricate shapes, slots, drilling holes, cutting and texturing. The specific texturing process known as Electro Discharge Texturing (EDT) generally has a multi rotary motor/ballscrew/slide/slideway arrangement in a small volume [1-3, 4]. The function being to focus as many electrodes into a given area as possible, given the limitations of the design constraints that is dominated by the physical size and volume of DC and or AC servomotors and the other kinematic elements required, to effect rotary to linear motion. Texturing is a process of creating irregularities, with regular or irregular spacing that tends to form patterns or texture on the surface. Texture contains roughness and waviness that can assist in providing the inherent quality of any subsequent paint finish, appearance and lifetime. Since the requirements of high precision and accurate machining of EDT applications never stop rising, much of the research has been concerned with the servo control feed drive level of precision, stability, dynamic response and surface profile of the textured products. Some authors have identified these issues [5-6]. Some authors have undertaken an investigation into the pre-ignition stage in EDM machining [7], to maintain topography, increase workpiece surface profiles and lifetime [8-9]. Others focused on detecting an abnormal 'arcing' process and investigated new techniques to prevent this [6], monitoring the effective size of the electrode in EDM machining [10], development of surface damage monitoring system for EDM machining [11]. In fact success in presenting a realistic solution to these issues has been limited. Therefore there was a need to develop a new servo control drive using innovative technology that could provide high precision, fast dynamic response and robust stability. Piezoelectric ultrasonic motor (USM) technology offers many opportunities in the field of high precision servo positioning control [12-13]. It has been used widely in both instrumentation and machine tool applications such as, EDM [2], EDT [3], micro-machining [1-3], artificial prostheses [14], auto focusing drives for single-lens reflex cameras, rotary supports for video cameras and artificial heart actuators [15]. These applications show that piezoelectric USM servo control systems can be more effective than DC and or AC servomotor drives whenever high and ultrahigh precision level of control is required. This is due to their high resolution, high stiffness, large output force, compactness and quick dynamic response despite their limited positioning ranges. These distinctive features presented a challenge to design a new servo control feed drive using piezoelectric USMs technology to improve EDT servo control system degree of precision, dynamic response, performance and extend its capabilities to include more accurate machining. The structure of piezoelectric ultrasonic servo drive is mainly depends on the industrial application requirements [1-3, 16-26]. Potentially they offer a significant flexibility for position and feed-rate control [28-30]. They have compact size, high force density, simple mechanical construction, low weight, slow speed without additional gear or spindle, high torque, non-magnetic operation, freedom for constructional design, very low inertia, fast dynamic time responses, direct drive, fine position resolution, miniaturization and noiseless operation. These criteria give them the potential to replace electromagnetic motors arrangements in a number of industrial applications [2-3]. Demanding and careful examination for these applications reveals that there are apparent shortcomings. The first shortcoming is in regard to the dynamic time response of the motor and its transfer function. While a piezo-ceramic element (typically Lead zirconate titanate (PZT)) expands in direct proportion to the magnitude of the applied voltage, the USM on the other hand accumulates those displacements over time. Therefore the transfer function of the USM, relating the magnitude of the driving signal to the displacement is an integrator [31-32] and this shows a delay in the dynamic response of the USM, but it is not nearly significant as that in an electromagnetic servomotor. The second shortcoming is that because motion is transmitted through a friction force it will have a dead band due to the friction. Often USM does not move until the input signal is greater than 10% of the maximum allowed voltage to overcome the friction. Such a dead band limits the ability of a USM to accelerate quickly and position accurately [2-3, 31-32].

The development life cycle of ultrasonic servo control drive has passed through a number of stages. The first stage focused on an investigation into the possible available high precision motors technology that could meet the EDT system needs and overcome its current servo control drive machining procedure teething issues. The second stage concentrated on the investigation into the ultrasonic motors technology design methodology working principles, advantages and disadvantageous. This was followed by the design and development of a linear high precision ultrasonic motor, finite element analysis of the motor structure, initial practical tests to obtain the motor technical operating parameters and major characteristics, design of its electronic drive, integration of the control drive units. The final stage focused on the test and validation of the developed servo control drive in EDM/EDT system platform.

## 2. Design, Analysis and Development of the Motor

The development and design process of the proposed USM has been considered application needs such as type of motion, degree of resolution, level of precision, travelling speed, output force required, load capacity, torque, compactness, integration of the parts into the frame of the motor, fabrications of the parts, maintenance and sustainability. The design process of the linear USM have passed through a number of phases, the first phase focused on the motor structure that could meet the EDT application requirements, structure, principles of motion, units design and integration into the motor frame.

### 2.1. Structure of the USM

The structure of the ultrasonic motor is shown in Fig.1. It consists of three main parts, which are the stator, rotor and sliding element. The stator is a single flexural vibrating transducer made from Lead Ziconate Titanate (PZT) piezoceramic material. The rotor is composed of the motor driving wheel and the shaft. The sliding element is made up of rectangular tube steel. The stator, rotor and sliding element jointly with the frame of the motor form the linear structure of the USM. The working principle of the motor is based on creating elliptical micro motions of surface points generated by superposition of longitudinal and bending vibration modes of oscillating structures [22-23]. By pressing the rotor against the driving tip of the stator, the micro motions are converted into a rotary and linear motion, through the friction between parts of the motor. However, to create a strong second bending vibration mode, the polarisation direction of the piezoelectric vibrator perpendicular to the electrodes, the piezoelectric ceramic vibrator was arranged as shown in Fig. 2. The longitudinal and bending vibration modes are coupled by asymmetry of the piezoelectric ceramic vibrator [21, 33-34]. The first surface of the piezoelectric transducer is segmented into four sub-surfaces, which were arranged electrically to provide two sub-electrodes, named A and B. The second surface is connected to the earth and is named electrode C. Then a single-phase AC signal with a wide frequency band is used to obtain the electrode natural operating frequency.

Driving the electrode A and C by a single phase AC signal with a frequency closer to the resonant frequency of the vibrator provide one direction of motion and switching to electrode B, change the bending vibration mode by a phase shift of 180 degrees which leads to reversing the direction of motions as shown in Fig. 3. Few authors have used these phenomena and succeeded to develop different structures to generate linear motion [22-23, 34-35]. Snitka [34] and Aoyagi et al [22] showed that the load of this type of motor depends on the contact point of the rotor, the dimension of the piezoelectric elements and material of the stator and the rotor. Snitka [34] proved that the pre-load pressing forces and friction between parts influence the degree of accuracy obtainable. Therefore, the material for the moving parts of the proposed motor has been carefully selected. It was also noticed that the slide element does not move until the excitation voltage reaches about half wave its maximum value, because a

single driving system with constant frequency is used to create both normal and thrust force. This reduces the fine micro resolution of the USM. The thrust force must overcome static friction between the motor parts, result of pre-load force, to allow relative motion between the stator and the rotor [28]. In the developed design a coil spring was used, to press the vibrating transducer against the rotor and enabled the pre-load force to be sensitively adjusted.

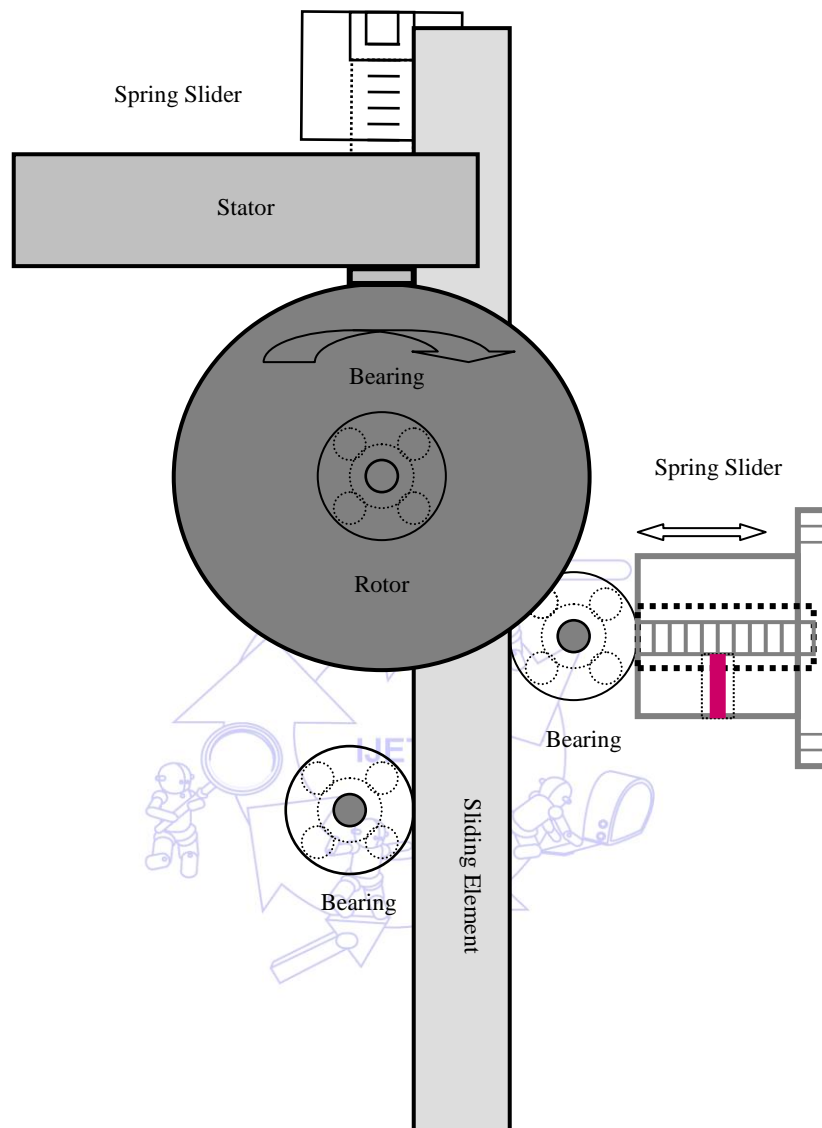


Fig. 1 Proposed standing wave linear ultrasonic motor structure using a single flexural rectangular vibration transducer for electro discharge texturing system industrial applications

## 2.2. USM Working Principles

The working principles of the proposed USM is utilised the standing wave vibrations standards, which it has a fixed wave length. The concept is to exploit two oscillation modes of vibration, to obtain desired motion of the piezoelectric vibrating transducer longitudinal and transverse vibration modes, one vibration produces a normal force, while the other vibration generates thrust force, which is perpendicular to the normal force, resulting in a micro elliptical trajectory of motion, at the vibration transducer tip, by attaching the stator tip to the rotor using a coil spring. The micro elliptical trajectory is converted into a rotary motion, as shown in Fig. 3. As the combination of two modes of vibrations creates a friction based driving force between the stator and the rotor at the contact tip, a movement in forward or backward direction was created depending on the

methodology used to electrify the piezoelectric ceramic transducer to generate two modes of vibrations. The linear motion was developed using the friction based driving force between the shaft and the sliding element of the motor as shown in Fig. 1.

2.3. USM Modelling and Analysis Using Finite Element

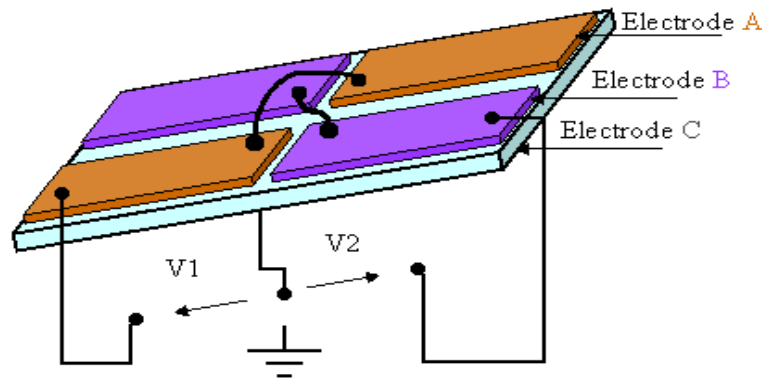


Fig. 2 Proposed ultrasonic motor stator arrangements and mechanism utilised to create two directions of motion using one single flexural vibration transducer

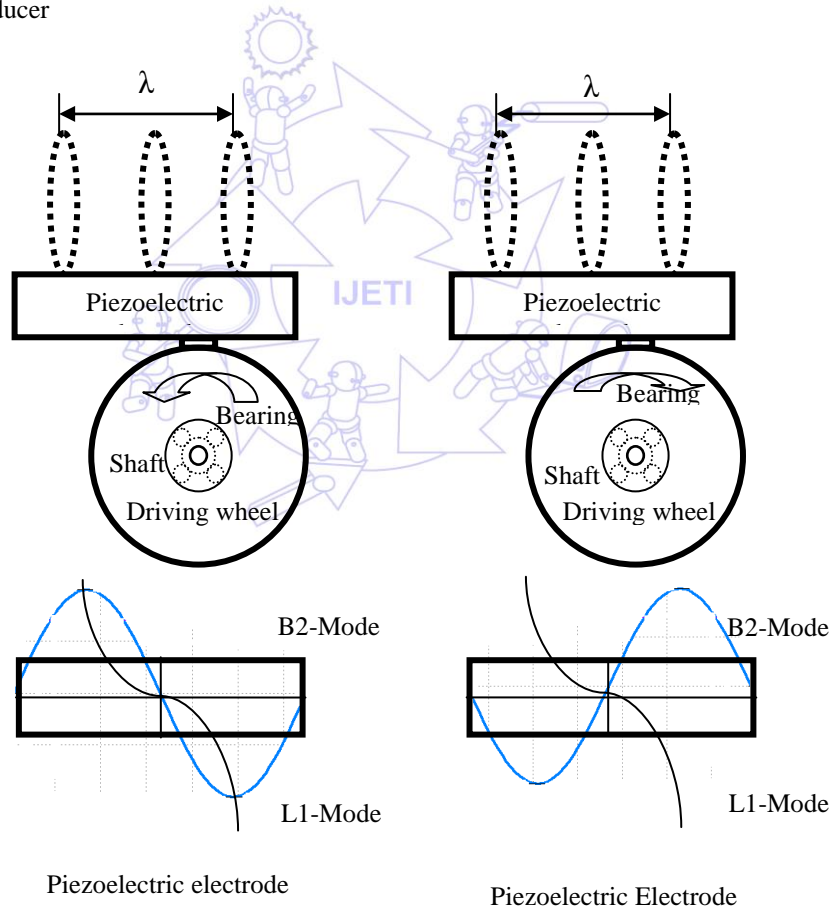


Fig. 3 Practice utilised to create bidirectional of motion using transverse longitudinal and bending vibration modes at a frequency close to the vibration mode

Modelling and analysis of ultrasonic motors is an essential step in the design and development life cycle of USM. They have many complicated and non-linear characteristics. There are two methods of modelling and analysis can be used to simulate and model piezoelectric USM's [36-39]. These methods are the analytical analysis and finite element analysis (FEA) method. In

the current developed USM development process, ANSYS FEA software was used, to examine the proposed motor structure, investigate the material vibration modes, identify the transducer material, and obtain the technical operating parameters.

It also helps to optimise the motor performance through investigating the variation of the displacement versus the frequency. Two types of FEA were used, model analysis and harmonic analysis. These offer two types of loads, the nodal and the pertaining to the element. In the nodal case the loads were applied to nodes of the element that do not have direct links with element properties.

An USM model was build, based on a full consideration of the motor boundary condition and EDT industrial application requirements. The stator was defined as the active element and the rotor was defined, as the passive element. Fig 4 (a) and (b) shows the variation of displacement of the stator versus the frequency, for rotary and linear structure, of the motor. It illustrates the change of displacement versus the frequency. It also shows the resonant frequency of the current model - 42.2 kHz. This is helped to determine the vibration amplitude, thrust force and optimise motor structure performance.

The analysis of motor linear arrangement model shows that there is some influences of the sliding element on the transducer deformation modes of vibration and the possible maximum displacement. The displacement of the transducer changed from 10.1125  $\mu\text{m}$  to 3.0999  $\mu\text{m}$ . This analysis enabled, to assess the motor possible generated amplitude of vibration, thrust force, material modes of vibration and the distribution of the vibration wave of the transducer. This helped to avoid design errors and avoid mishandling of the material deformation. Material deformation can produce a jerking effect that affects the resolution and degree of accuracy of the motor. Consequently, it could restrict the potential applications of the proposed USM motor and the ultrasonic servo drive fine position as a whole. The motor model-vibration modes for different input signal were determined. Figures 5 and 6 show the two modes of vibration for the motor, the transverse bending mode and longitudinal mode, at the drawn operating frequency.

#### 2.4. Design and Development of the USM Components

The dimensions of the proposed USM parts was mainly based on the frequency ratio between the longitudinal mode  $f_L$  and the bending mode  $f_B$ ,  $f_L / f_B = 2.0$ , and  $d/l = 0.1$ , as the internal nonlinear coupling of parametric vibration between two resonance modes was generated under these conditions [6]. The capacitance ratio and direction of vibratory displacement was also considered.

Using the USM models shown in Figures 7 (a) and 7 (b), the relation between the torque  $T$  and various acting forces on the rotor components this gives the following relationship:

$$T = F_R \frac{D}{2} = F_r \frac{d}{2} \quad (1)$$

Where,  $F_R$  is the micro elliptical force produced using vibration transducer,  $F_r$  is the driving force transferred to the shaft using the following torque factor relationship  $A_r = D/d$ . Where,  $D$  is the diameter of the driving wheel and  $d$  is the diameter of the shaft.

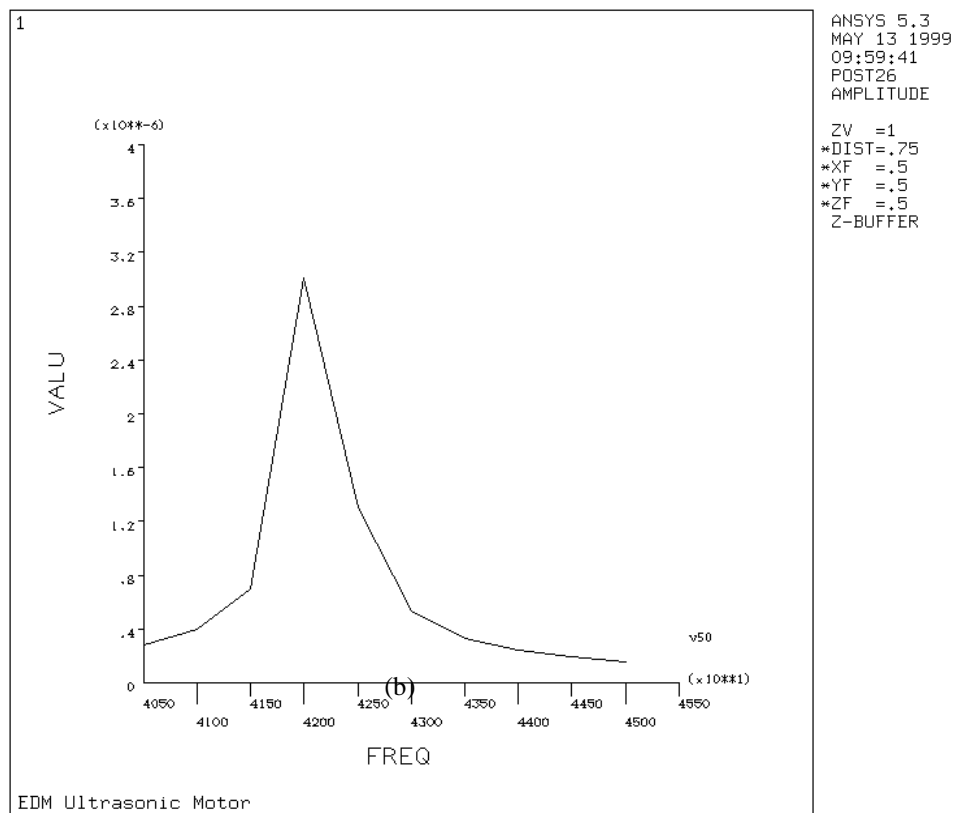
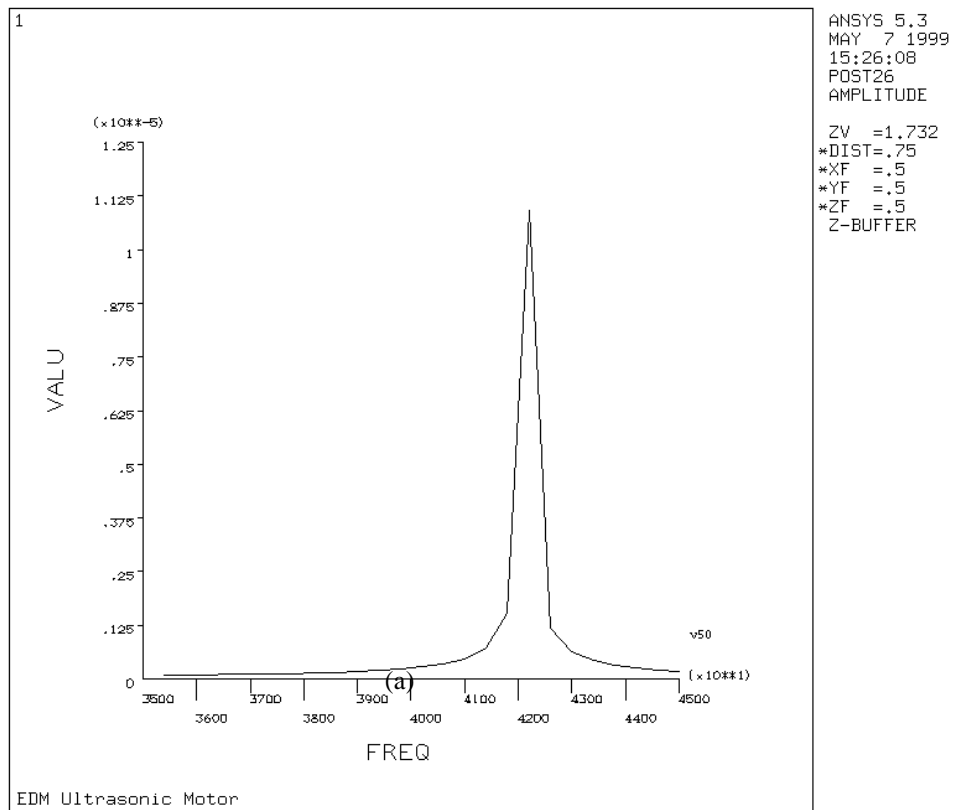


Fig. 4 The ultrasonic motor stator displacement amplitude vs. the frequency for the developed USM (AC 50V) (a) for rotary USM structure and (b) for linear USM structure

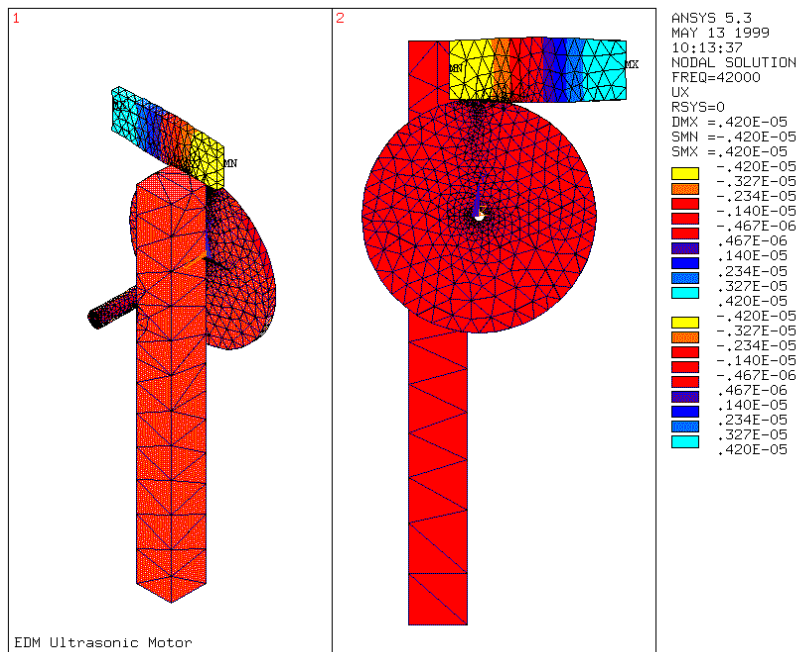


Fig. 5 Ultrasonic motor linear structure model FEA transverse bending vibration mode (Frequency 42,200Hz and AC 50V)

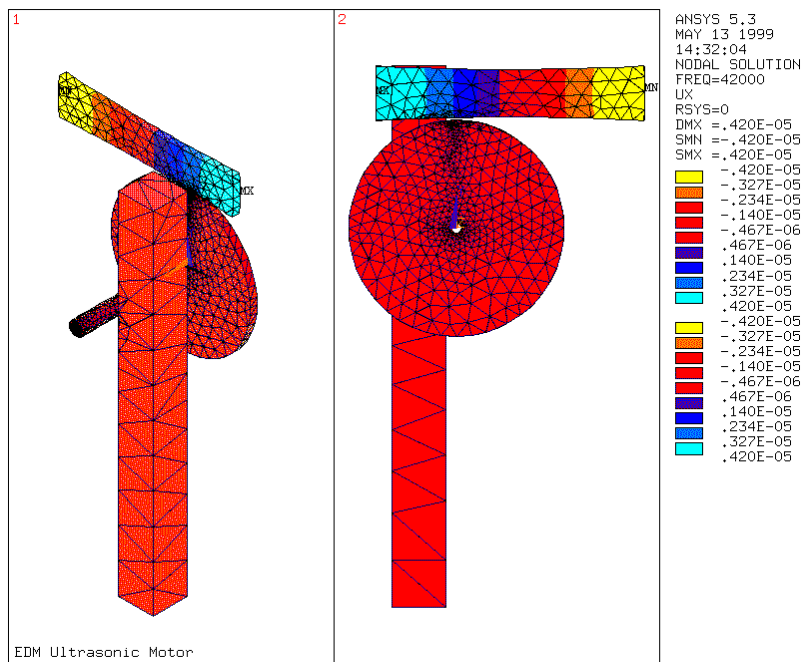


Fig. 6 Ultrasonic motor linear structure model FEA transverse longitudinal vibration mode (Frequency 42,200Hz and AC 50V)

The torque factor of the USM and the diameter of the rotor (driving wheel and the shaft) were obtained. The transferred force to the shaft was determined using the following torque factor relationship:

$$F_r = F_R \frac{D}{d} \tag{2}$$

This relationship shows that the torque factor  $A_r$  has to be carefully considered during the design process of the USM since it influences the efficiency of the driving force produced by the vibration transducer, the resolution of the motor and maximum travelling speed.

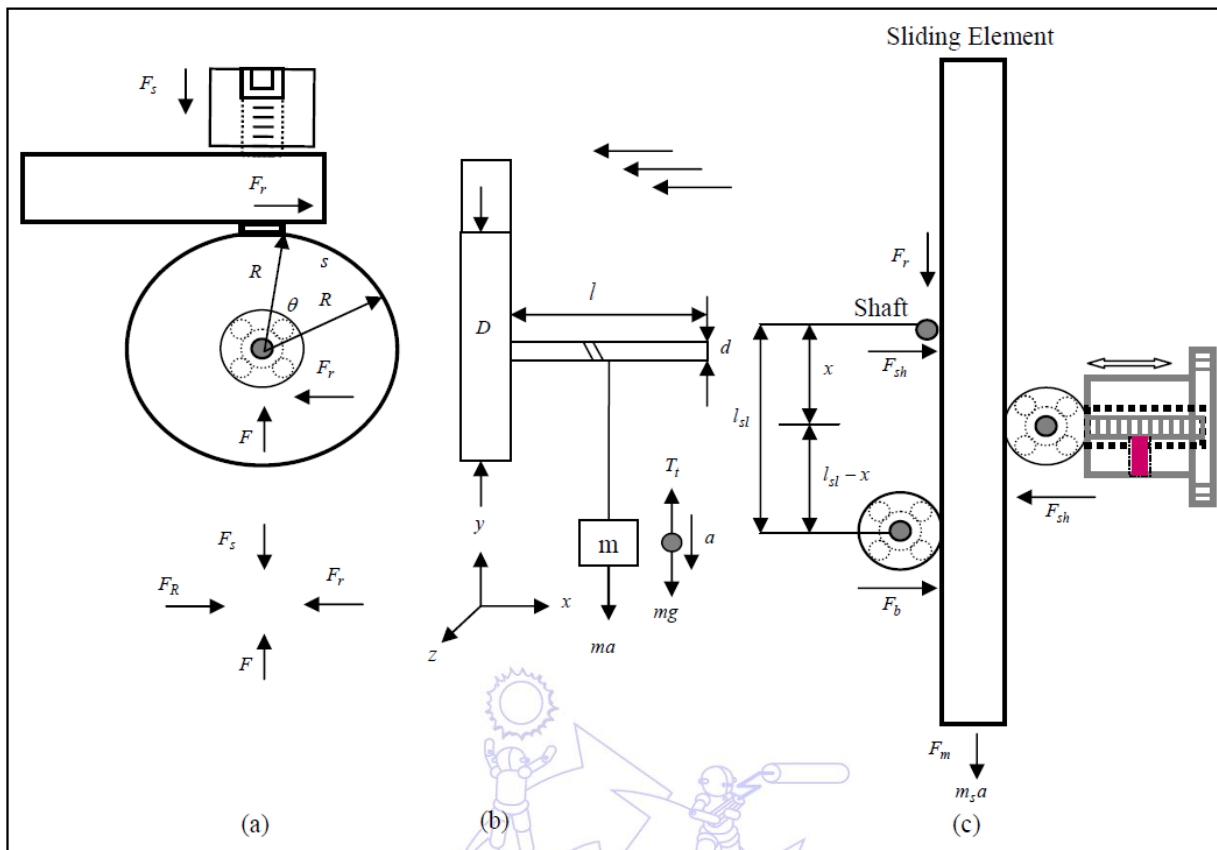


Fig. 7 Dynamic models utilised to design actual dimensions of the ultrasonic motor parts and optimise the bearing preload force on the motor linear structure

The length of the shaft  $l_s$  was determined according to the allowable ratio of the  $l_s/d_s$ , where  $d_s$  is the diameter of the shaft. This is to meet the conceptual view of the design for the proposed motor construction. This considered the properties of the material used to produce the shaft and the moment of inertia of the rotor. The moment of inertia of the rotor was considered to be small for fast dynamic time response and to obtain a maximum efficiency of the transferred driving force. The pre-load force acting in the shaft and locations of bearings of the sliding element was determined using the dynamic model shown in Fig. 7.

$$\begin{aligned} \sum F_x &= 0.0 \\ F_{sb} &= F_{sh} + F_b \end{aligned} \tag{3}$$

Where:  $F_{sb}$ ,  $F_b$ ,  $F_{sh}$  are the side spring slider, bearing and shaft acting forces, respectively

From the model shown in Fig. 7-c, the bearing acting force  $F_b$  was obtained from the following relationship:

$$F_{sb} X = F_b l_{sl} \tag{4}$$

Consequently the bearing acting force was found to be:

$$F_b = F_{sb} \frac{X}{l_{sl}} \tag{5}$$

Substituting  $F_b$  into slider acting force:

$$F_{sb} = F_{sb} \frac{X}{l_{sl}} + F_{sh} \quad (6)$$

Then the shaft acting force was determined using the relationship (7):

$$F_{sh} = F_{sb} \left(1 - \frac{X}{l_{sl}}\right) \quad (7)$$

In the design process of the USM the side spring slider was located in the middle between the shaft and opposite side bearing, to keep the acting force on the shaft, as minimum as possible (see Fig. 7 (c)). The acting force on the shaft in this case was found to be half the slider pre-load acting force. Four pins and an interchangeable coil spring was used to house the vibration transducer as shown in Fig. 7 (a). The four pins were used to prevent interference transducer modes of vibrations. The spring was used to support the vibration transducer at the vibration tip. It was also used to keep the stator and rotor in contact. This enabled the vibration transducer to transfer the micro elliptical force, into rotational and linear motion using the friction between the USM parts. The optimum pre-load acting force was determined, by observing the USM travelling speed versus various forces, at the identified operating parameters i.e. voltage, current and frequency. It was clearly noticed that mishandling of the pre-load acting force influences the motor resolution, stiffness and torque. Two guide-ways were also designed and fixed to the top and bottom of the USM frame. This is to prevent the sliding element plane motion. Plane motion would affect the accuracy of the USM. The frame of the motor was part of the concept and was designed with a reliable layout to ensure compactness of the design, easy to integrate and maintain the parts of the USM. Fig 8 illustrates the USM and fabricated prototype.

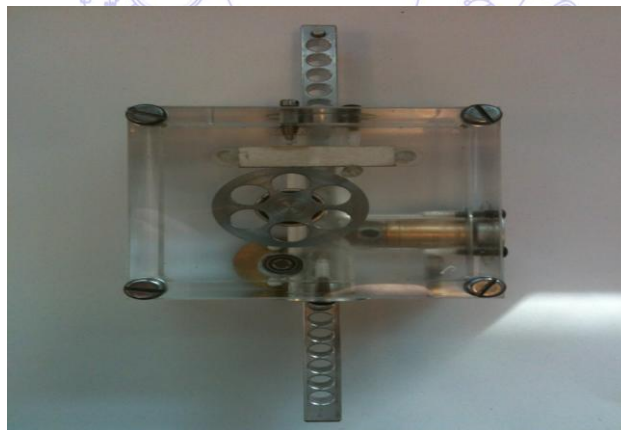


Fig. 8 Actual fabricated prototype of ultrasonic motor using a single piezoceramic PZT ultrasonic flexural vibration transducer

### 2.5. Experimental Test of the Developed USM Prototype

The parts of the developed USM prototype were assembled into the USM frame and series of experimental tests carried out. This was aiming to examine the definitive characteristics of the fabricated prototype and EDT industrial application requirements. Initial integration showed that there were some teething problems. These included irregular rotational and linear motion. These problems arise due to the inaccuracies in the manufacture of the parts of the USM. The irregular rotational speed was due to deviations on the roundness of the driving wheel and irregular travelling speed was from deviations in roundness of the shaft. The roundness of the driving wheel and the shaft were re-machined and retested. The concentricity of the produced

parts, such as the rotor, was also tested and showed no error. The parts were reintegrated into the frame of the USM and a series of experimental test were conducted, to measure the characteristics of the USM. Fig 9 shows the block diagram of the test rig and Fig. 10 shows the actual system used to examine the prototype. An off-shelf piezoelectric driver was used, to supply the vibrating transducer with the AC voltage. Various shapes of AC signal including sinusoidal, saw-tooth and square wave. A display unit, which comprised of a digital oscilloscope and PC computer, was deployed to trace the signal and determine the USM operating parameters. The travelling speed of the USM was measured via a speedometer. An electro microscope was used to measure the fine resolution of the USM. A programmable switching unit interfaced with a PC computer was used to control the USM directions of motion and to analyse the measured characteristics.

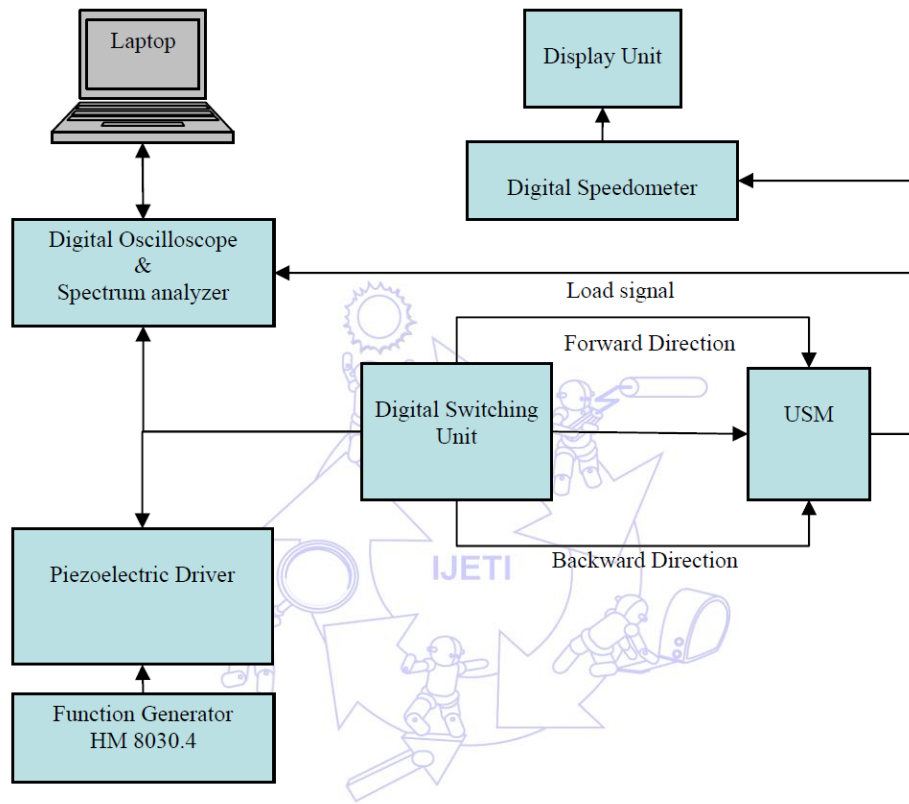


Fig. 9 Block diagram of the test rig arrangement used to test and measure the characteristics of the developed ultrasonic servo drive prototype

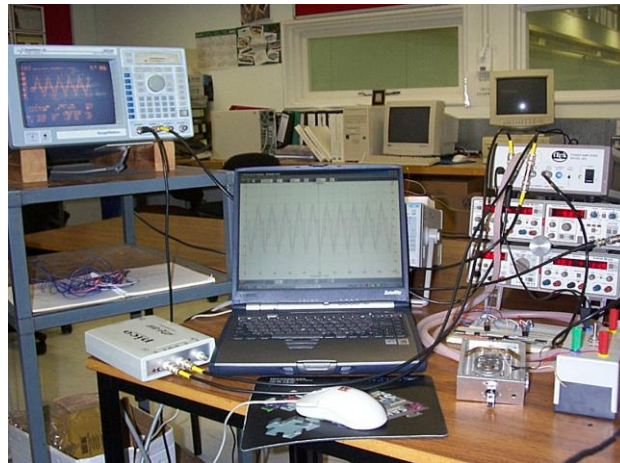


Fig. 10 Actual test rig arrangement used to test and measure the characteristics of the developed ultrasonic servo drive prototype

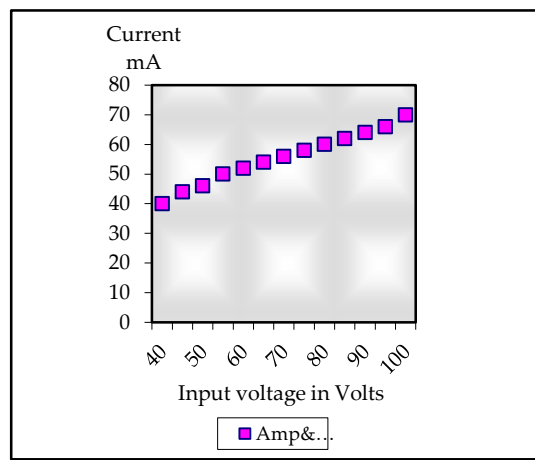


Fig. 11 The variation of the current in mA vs. input voltage of the developed USM prototype (no-load applied)

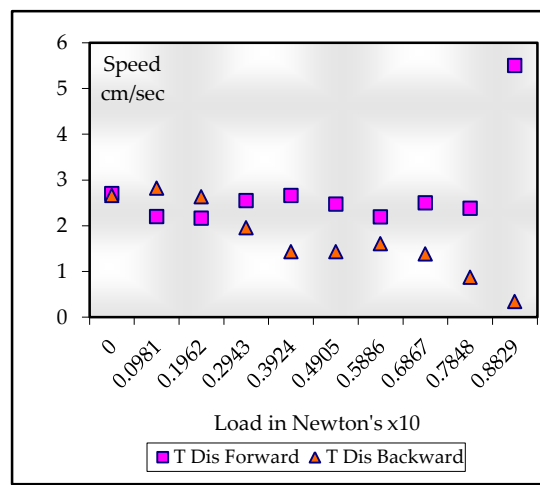


Fig. 12 The variation of the travelling speed in cm vs. applied load of the developed USM prototype

The operating parameters were measured using the same arrangement shown in utilised during the FEA. The electrodes A and B were connected to a single phase AC power source, with a wide range of amplitude and frequency. A switching unit were used to regulate the AC input power for A, B and C electrodes. Fig. 11 shows the relationship between current and voltage of the USM prototype. This help to identify the nature of the USM load. It also helped to define the USM operating voltage and current. This was found to be: voltage: 50 to 100 volts and current: 50 to 100 milliamperes. Then the travelling speed versus the amplitude and frequency of the AC input signal measured. This was achieved as follows: the frequency of USM driver was being altered incrementally. The speed of the USM was measured for each increment. It was noticed that during this process that the speed of the USM increased as the frequency of the driver increased. At one stage the USM reached a maximum speed and then the speed started to decrease dramatically. This process allows to obtaining the relationship between the travelling-speed versus the operating frequency. This shows that the operating frequency for the developed prototype for no-load was 40.7 kHz. The travelling speed versus the input voltage also established. It shows that the developed USM was able to provide a travelling speed of 28.0mm/s, and a resolution on the order of micrometers. The variation of the travelling speed versus the applied load was also measured at various loads, and is shown in Fig. 12. This showed that the developed prototype was able to carry a load up to 1.8Newton which meets the requirements for electro discharge texturing system industrial applications. The developed prototype had two directional of motion with un-similar characteristics as shown in Fig. 12. It had a wide range of frequency

which enabled to control the travelling speed of the motor. Varying the frequency or the amplitude of the input signal controlled the traveling speed of the USM.

### 3. Architecture of the USM Electronic Driver

The design process of the developed USM piezoelectric driver passed through few steps. First the technical operating parameters have been identified using off-shelf piezoelectric driver unit. This is allowed to define the USM operating frequency (40.7 KHz), voltage (50: 100 volt) and current (50: 100-mamp). Then the right design approach has been identified for the driver circuit. The approach is to use two stages. The first stage is a DC/DC converter that is boost 18 volt input to 80 volt. The second stage is a piezo amplifier which consists of four output transistors, push-pull and bridge connected in order to achieve maximum amplitude. The input signal to the amplifier is generated by an oscillator, op-amp circuitry. The output from the oscillator is low pass filtered in order to achieve a sine wave signal. The sine wave is then voltage amplified by a transistor to approx 50V before it is connected to the USM.

### 4. Experimental Test and Validation of the Servo Control Drive in EDT

The ultrasonic Servo control drive has been incorporated, tested and validated in Electro Discharge Texturing System platform. The developed system evaluated compared to the existing system using AC and DC servo feed drive. This included, an investigation into the stability of the system, capability of control, processing time and surface finish of the textured products. This was carried out using various electro-texturing parameters, including level of current, on/off time and duty cycle. Fig 13 shows the system installed in EDT A ELEKTRA R-50 ZNC model.

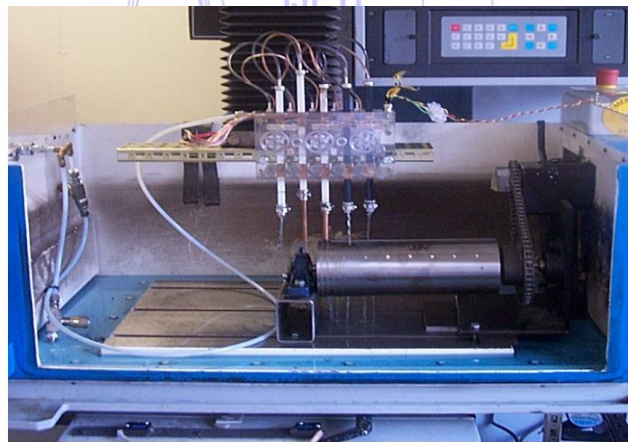


Fig. 13 The developed ultrasonic servo drive installed in the EDM/EDT machine (A ELEKTRA R-50 ZNC model)

### 5. Analysis and Discussion

The Electro discharge Texturing system is a variation of the Electro discharge machining process. As with electro discharge die sinking, ED wiring, ED sawing and ED grinding, the major difference is in the configuration of the main elements of the machine. Here an experimental investigation into the current EDT-system and the developed control system using piezoelectric ultrasonic drive was conducted. The current system, using DC servo feed drive, was used for texturing different areas using various electro-machining parameters. Then the developed system, using piezoelectric ultrasonic feed drive, was used for machining using the same electro-machining parameters and similar conditions. Texturing different sampled was carried

out using the EDT machine. The levels of current, on-off time and duty cycle were used as main electro-machining parameters. The other machining parameters were selected as follows: The feed rate of the system in the case of auto position was 0.656 mm/sec, speed of the roll was 6 rpm, SEN = 1:3 [Sensitivity of Z-axis speed], ASEN = 3-9 [Antiarc sensitivity], TW = 1.0  $\mu$ sec [Sparking time], T = 0.5  $\mu$ sec [Lifetime], Vg = 38: 50 volts [Gap voltage], Ig = 5 amperes [Gap current], Ib = 0.0 [Prepulse spark current], POL=-ve [Polarity of machining] and Fp=0.2 bar [Flushing pressure]. The feed rate in the case of the piezoelectric ultrasonic control system was of the order of 5.1 mm/sec. An evaluation for both control systems was also conducted. This included stability of the system, surface profiles (roughness, Pc peak/cm), capability of the system to monitoring and control of the inter-electrode gap, and safety of machining process.

The stability of the EDT-system can be measured from the inter electrode gap voltage and current in addition to the control signal obtained from the system control unit. Therefore the feedback signal and inter-electrode gap voltage variation were obtained at various electro-machining parameters. Figures 14 and 15 illustrate the variations of these signals for various electro-machining parameters for both control systems. It shows the indication of the stability of machining for a period of 10 seconds. Fig 14 shows these variations for the existing control system using electric motor. Here it is notable that there is a clear instability on the feedback signal and the inter-electrode gap. Fig 15 shows the variation in the feedback control signal and inter-electrode gap voltage for the developed system. This shows the stability of machining, remarkable reduction in the arcing and short-circuiting processes, which in turn may lead to a clear reduction in the machining time when compared to the current system. It was also observed, during this investigation, that the increment in the required level of current had no major influence on the stability in the case of the piezoelectric USM system as in the case of the electric motor. Two factors showed an effect on the machining process, namely the sensitivity and the anti-arc factor. The capability of changing the machining parameters during machining process was used in this case to select the optimum values, which provided a stable machining. It was noticed, that mishandling the sensitivity and anti-arc factors produced jerking effect, and lead to unstable machining which in turn increased the arcing and short-circuiting process. The arcing and short circuit processes led to poor surface profiles and increased the machining time of the process. This was clear in the case of the electric servomotor control system rather than the developed control system using piezoelectric USM. A scanning electron microscopic investigation into the textured surface using EDT-system for both systems of control using current and developed system were carried out. Figures 16 and 17 show the scanning electron microscope image of the textured surface profiles using both control systems. These figures show the investigations into the surface profiles machined using a different duty cycle. It shows noticeably how the duty cycle was used to control the machined surface finish. It also shows the difference between the surface profiles obtained using piezoelectric USM system and electric servomotor system. It can be seen that there is a smooth surface obtained using the developed system. Figures 18 and 19 show a close investigation into the textured surface profiles for cross-section area 20 microns. This shows evidently the smooth surface finish obtained using piezoelectric USM control system compared with the EMM control system.

A Taylor Hobson measuring system for surface finish was used to measure the roughness and peak count of the various machined areas along the roll. This was carried out a few times for each sample and the average of the degree of texture was determined. The relationships between measured degree of roughness and peak count of the textured surfaces using both systems for control and various electro-machining parameters are shown in figures 20, 21, 22 and 23. Figures 20 and 21 show the variation of the degree of roughness, versus peak current, and on-off time. This shows a close agreement with the previous results obtained in this area of machining. It can be seen that the degree of roughness of the textured surface using both techniques of control is increased as the peak current and the on-off time increased. There was a small deviation in the degree of roughness of the bands machined using the developed system when compared to the existing electric servomotor system [40-41].

Figures 22 and 23 show the variation of the peak count versus the peak current and on-off time. Here it can be seen that the peak count decreased as the peak current and on-off time increased. These illustrates the potential advantages of the developed servo control drive using ultrasonic motor technology which are direct drive, fine position, high resolution, dynamic time response and compact size in comparison to a DC and or AC servomotors. The drive also offers the same kinematics capability as a rotary motor/ballscrew/slide/slideway arrangement and is controllable within the limits that DC/AC servos operate [42-43]. This is in addition to its compactness, sustainable design structure and low cost compared with any other motor technology arrangement. This has brought the fruition to the EDT servo control drive and overcomes the aforementioned teething issues.

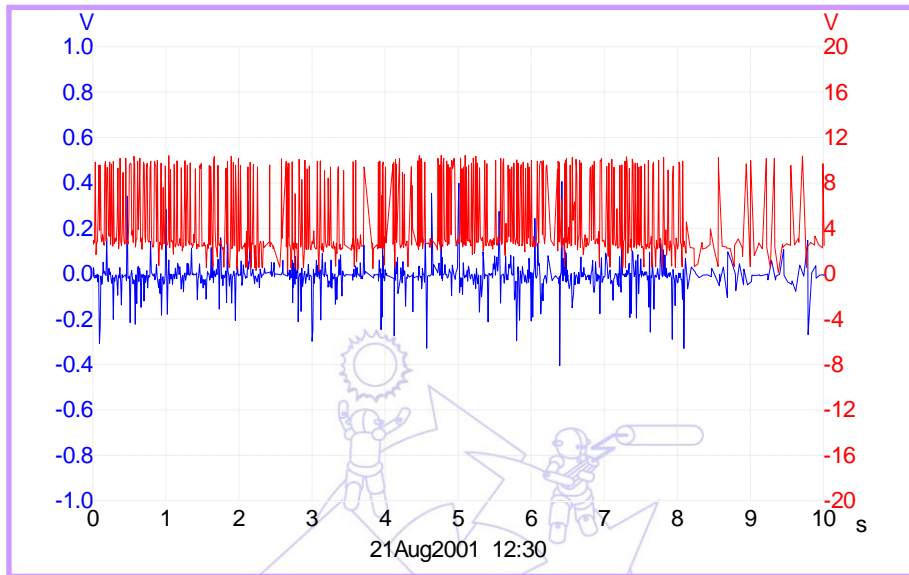


Fig. 14 Feedback control signal and inter-electrode gap voltage variation for EDT machining using the current DC servo control system [gap current 5A, gap voltage of 38 volts & duty cycle 8μsec]

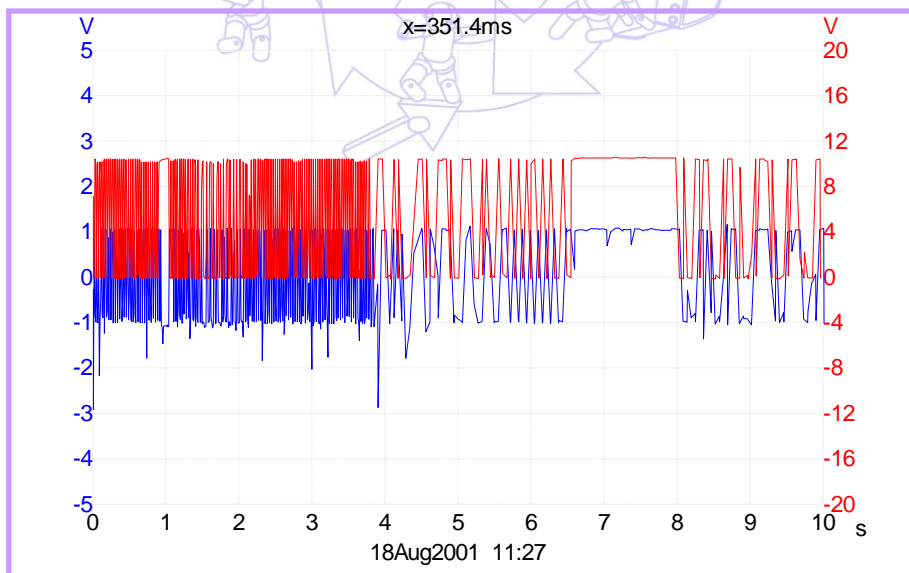


Fig. 15 Feedback control signal and inter-electrode gap voltage variation for EDT machining using the developed piezoelectric USM control system [gap current 5A, gap voltage of 38 volts & duty cycle 8μsec]

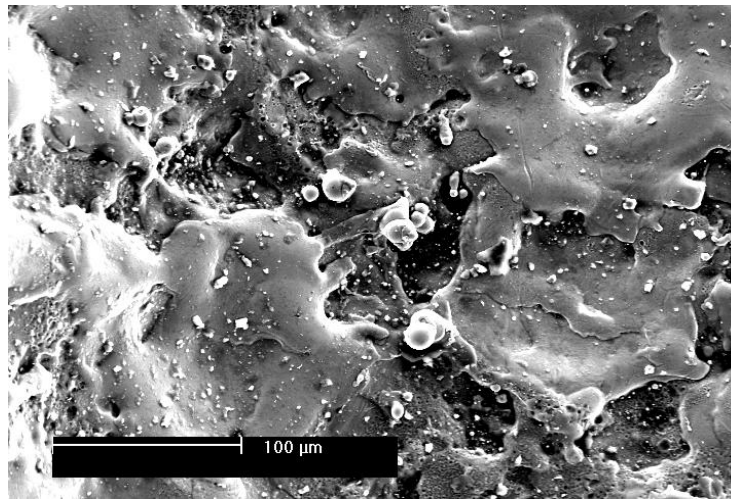


Fig. 16 EDT surface finish obtained using DC servo control feed system using current level of 6 amperes, 'on' time of 50 μsec, duty cycle of 4 μsec

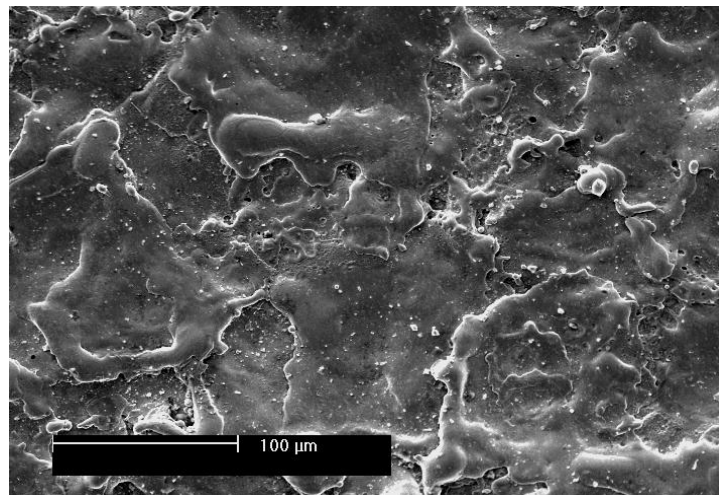


Fig. 17 EDT surface finish obtained using USM servo control feed system using current level of 6 amperes, 'on' time of 50 μsec, duty cycle of 4 μsec

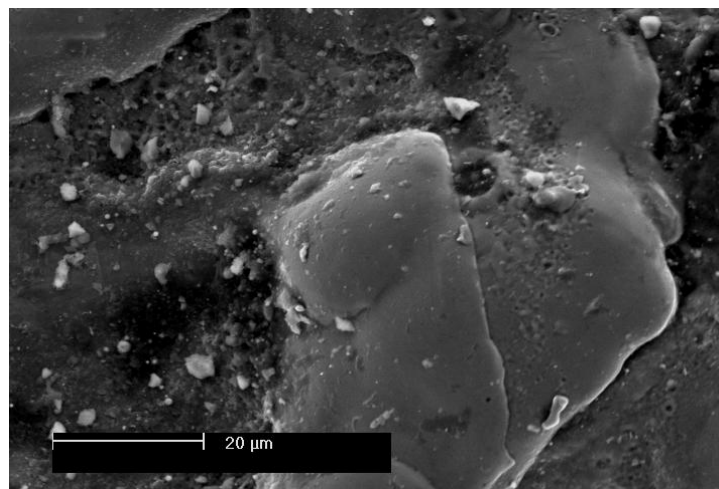


Fig. 18 EDT surface profiles from the DC control system and operating parameters, current of 6 amperes, 'on' time of 50 μsec and duty cycle of 12 μsec

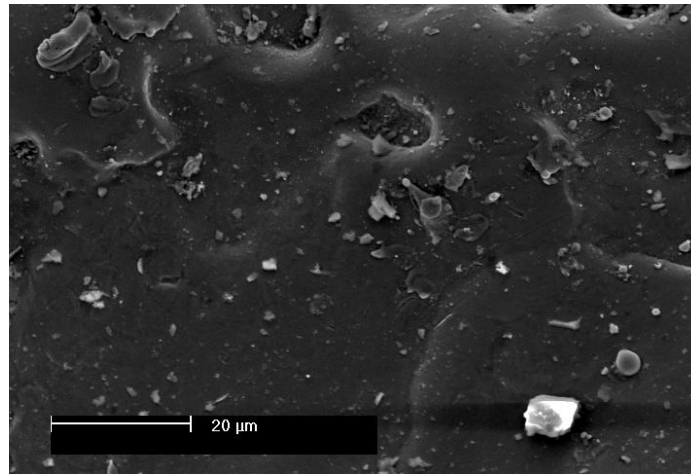


Fig. 19 EDT surface profiles from the USM control system and operating parameters, current of 6 amperes, ‘on’ time of 50 μsec and duty cycle of 12 μsec

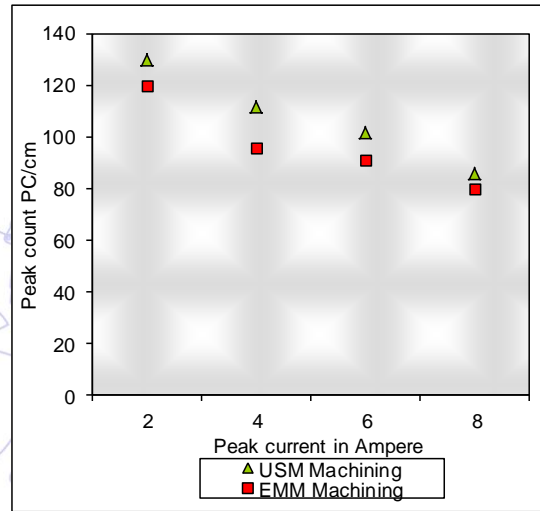
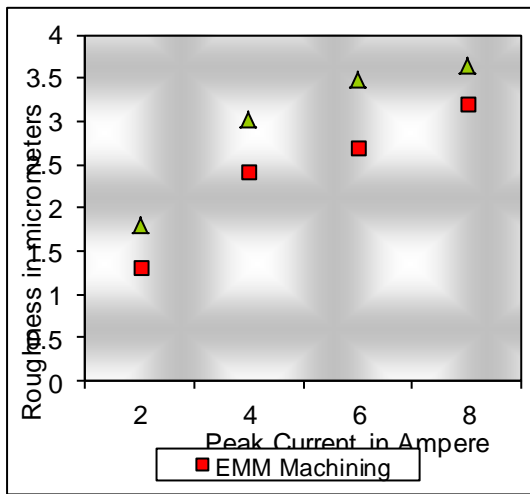


Fig. 20 The measured degree of roughness vs. the machining parameters for both systems of control using DC servomotor and USM technology

Fig. 21 The variation of the measured peak count vs. various peak current for both systems of control using DC and USM technology

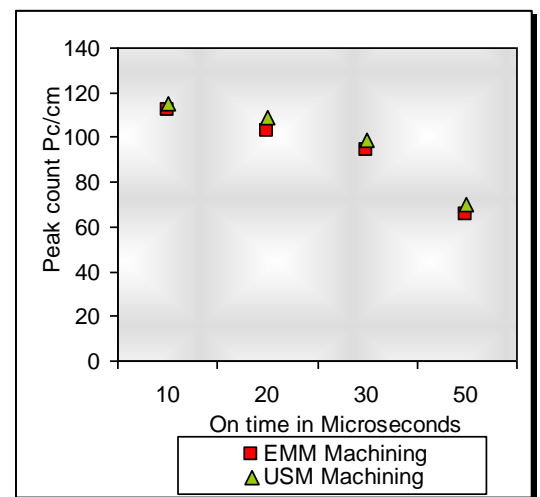
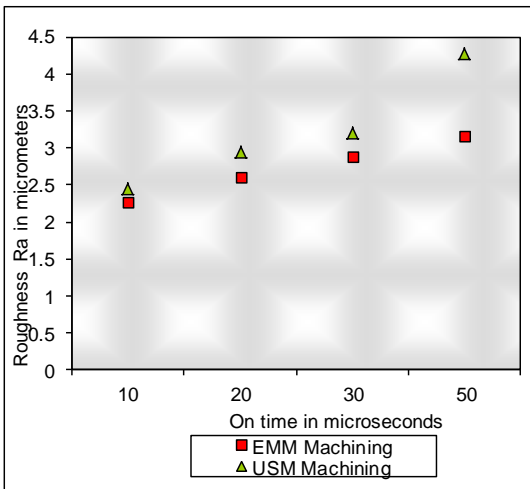


Fig. 22 The variation of the measured degree of roughness vs. on time for both systems of control using DC and USM technology

Fig. 23 The variation of the measured peak count vs. on/off time for both systems of control using DC and USM technology

## 6. Conclusions

A new ultrasonic servo control feed drive for EDT System industrial application has been developed. The developed servo control drive offers high level of precision, high resolution, high stiffness, large output force, compactness and quick dynamic response despite its limited positioning ranges. These features overcomes the current EDT servo control teething issues and improve the system level of precision, stability, dynamic response and surface profile of the processed products. FEA has been used in the ultrasonic servo drive design development process. It has been used to examine the USM structure, material deformation and determine the operating parameters of the USM. A prototype of the ultrasonic servo drive was fabricated and the experimental tests to check the drive reliability for EDT System carried out. The results showed that the developed prototype operating parameters for no-load were: frequency: 40.7 KHz, voltage: 50: 100 voltage and current: 50: 100 m-amperes. The test also showed that the drive is able to provide: a reversible directional of motion, no-load travelling speed equal to 28.0mm per second, maximum load of 1.8 Newton, a resolution  $<50\mu\text{m}$  and a dynamic response in the order of microseconds. The developed ultrasonic servo drive has been tested and validated in EDT System platform. The experimental results showed that a significant improvement in the stability of machining when compared to the existing system using DC/AC servomotor. This was verified by examining the electrode movements, the inter-electrode gap voltage, current and feedback control signals.

The electron microscopic investigation into the surface profiles using both systems of control showed that there was a visible improvement in the surface profiles textured using the USM servo control system. A notable reduction in the arcing and short circuit process was also observed. The relationship between the electro texturing parameters and surface profiles roughness was obtained and this showed a close agreement with the existing system with minor deviation in the degree of roughness. These results demonstrate the ability of the developed system using the ultrasonic servo control drive to be implemented in various industrial applications wherever, a high level of precision, micro-resolution and fast dynamic time response is required. It presented a breakthrough in the EDT system technology and has made good economic and commercial impacts since the system have been implement by a number of companies around the world.

## Acknowledgements

The author would like particularly to thank, Professor J A Knight and Professor R. Bansevicius for their help, support and constructive discussion throughout this research. My deepest thanks also goes to Professor S M Ahmed for his professional guidance and endless support.

## References

- [1] M. Shafik, "Computer Aided Analysis and Design of a New Servo Control Feed Drive for EDM using Piezoelectric USM," PhD Thesis, De Montfort University, Leicester, UK, 2003.
- [2] M. Shafik and J. Knight, "An investigation into electro discharge machining system applications using ultrasonic motor," Proceeding of IMC International Conference, Aug. 2002, pp. 28-31.
- [3] M. Shafik, J. Knight and H. Abdalla, "Development of a new generation of electrical discharge texturing system using an ultrasonic motor," 13th International Symposium for Electromachining, ISEM, May 2001, pp. 9-11.
- [4] J. Simao, D. Aspinwall, F. El-Menshaway and K. Ken Meadows, "Surface alloying using PM composite electrode materials when electrical discharge texturing hardened AISI D2," Journal of Materials Processing Technology, vol. 127, pp. 211-216, 2002.
- [5] A. Behrens, and J. Ginzl, "An open numerical control architecture for electro discharge machining," 13th international symposium for Electromachining, ISEM, May 9th to 11th, 2001.

- [6] A. Behrens, J. Ginzel and F. Bruhns, "Arc detection in electro-discharge machining," 13th international symposium for Electromachining, ISEM, May 9th to 11th, 2001.
- [7] H. P. Schulze, M. Lauter, G. Wollenberg, M. Storr and W. Rehben, "Investigation of the pre-ignition stage in EDM," 13th international symposium for Electromachining, ISEM, May 9th to 11th, 2001.
- [8] D. Aspinwall, Y. Kasuga and A. Mantle, "The use of ultrasonic machining for the production of holes in  $\gamma$ -TiAl," 13th international symposium for Electromachining, ISEM, May 9th to 11th, 2001.
- [9] T. Satsuta and K. Hirai, "Surface modification using electrode transfer induced by discharge in gas," 13th international symposium for Electromachining, ISEM, May 9th to 11th, 2001.
- [10] I. J. Valentin and M. Junkar, "Monitoring of the effective size of the electrode in EDM," 13th international symposium for Electromachining, ISEM, May 9th to 11th, 2001.
- [11] H. Obara, T. Magota, T. Ohsumi and M. Hatano, "Development of surface damage monitoring system for EDM," 13th international symposium for Electromachining, ISEM, May 9th to 11th, 2001.
- [12] F. Zhang, W.S. Chen, J.K. Liu, Z.S. Wang, "Bidirectional linear ultrasonic motor using longitudinal vibrating transducers," IEEE Trans. Ultrason. Ferroelectr. Freq. Control., vol. 52, pp. 134-138, 2005.
- [13] Y. Izuno, T. Izumi, H. Yasutsune, E. Hiraki and M. Nakaoka, "Speed tracking servo control system incorporating travelling-wave-type ultrasonic motor and feasible evaluations," IEEE Transactions on Industry Applications, vol. 34, pp. 126-132, January-February, 1998.
- [14] Y. Izuno, and M. Nakaoka, "Ultrasonic motor actuated direct drive positioning servo control system using fuzzy reasoning controller," Electrical Eng. in Japan, vol. 117, pp. 74-84, 1996.
- [15] Hosoe, "Ultrasonic motors for auto-focusing lenses," Choonpa Techno, vol. 1, pp. 36-41, 1989.
- [16] K. Furutani, and A. Furuta, "Evaluation of driving performance of piezoelectric actuator with current pulse," 10th IEEE International Workshop on Advanced Motion Control, March 2008, pp. 26-28, pp. 387-392.
- [17] F. Zhang, W. Chen, J. Lin, and Z. Wang, "Bidirectional linear ultrasonic motor using longitudinal vibrating transducers," IEEE Transactions on Ultrasonics, Ferroelectrics and Frequency Control, vol. 52, pp. 134-138, 2005.
- [18] Y. Chen, K. Lu, T.Y. Zhou, T. Liu, and C.Y. Lu, "Study of a mini-ultrasonic motor with square metal bar and piezoelectric plate hybrid," Jpn. J. Appl. Phys., vol. 45, pp. 4780-4781, 2006.
- [19] X. Li, W.S. Chen, X. Tang, and J.K. Liu, "Novel high torque bearingless two-sided rotary ultrasonic motor," Journal of Zhejiang University - Science A, vol. 8, pp. 786-792, 2007.
- [20] A. Frangi, A. Corigliano, M. Binci, and P. Faure, "Finite element modelling of a rotating piezoelectric ultrasonic motor," Ultrasonics, vol. 43, pp. 747-755, 2005.
- [21] M. Aoyagi, Y. Tomikawa and T. Takano, "Ultrasonic motors using longitudinal and bending multimode vibrators with mode coupling by external additional asymmetry or internal nonlinearity," Japanese J. of Applied Physics part 1, vol. 31, pp. 3077-3080, 1992.
- [22] M. Aoyagi and Y. Tomikawa, "Ultrasonic motor based on coupled longitudinal-bending vibrators of a diagonally symmetry piezoceramic plate," Electronics and Communications in Japan, vol. 79, pp. 60-67, 1996.
- [23] K. Chiharu et al., "Effect of the pressing force applied to a rotor on Disk type ultrasonic motor driven by self oscillation," Japanese journal of applied Physics, vol. 37, pp. 2966-2969, 1998.
- [24] M. Shafik, "Computer Simulation and Modelling of Standing Wave Piezoelectric Ultrasonic Motor Using Flexural Transducer," ASME 2012 International Mechanical Engineering Congress and Exposition, Houston, TX, USA, 2012.
- [25] M. Shafik, "An Investigation into the Influence of Ultrasonic Servo Drive Technology in Electro Discharge Machining Industrial Applications," ASME 2012 International Mechanical Engineering Congress and Exposition, Houston, TX, USA, 2012.
- [26] Y. Ming, and P. W. Que, "Performance estimation of a rotary traveling wave ultrasonic motor based on two-dimension analytical model," Ultrasonics, vol. 39, pp. 115-120, 2001.
- [27] L. Lebrun, et al., "A Low-cost piezoelectric motor using a nonaxisymmetric Mode," Smart Mater. Struct., vol. 8, pp. 469-475, 1999.
- [28] T. Takano, Y. Tomikawa and C.K. Takano, "Operating characteristics of a same-phase drive-type ultrasonic motor using a flexural disk vibrator," Japanes J. of Applied physics part 1- 1999, vol. 38, pp. 3322-3326, 1999.
- [29] S. He, W. Chen, X. Tao and Z. Chen, "Standing wave bi-directional linearly moving ultrasonic motor," IEEE Transactions on Ultrasonics, Ferroelectrics and Frequency Control, vol. 45, pp. 1133-1139, 1998.

- [30] Newton D., Garcia E. and Horner G. C., "A Linear piezoelectric motor," *Smart Materials and Structures*, vol. 6, pp. 295-304, 1997.
- [31] B. Zhang and Z. Zhenqi, "Developing a linear piezomotor with nanometer resolution and high stiffness," *IEEE/ASME Transaction on Mechatron*, vol. 2, pp. 22-29, 1997.
- [32] J. Tal, "Servomotors take piezoceramic transducers for a ride," *Machine Design*, vol. 71, pp. 1-3, 1999.
- [33] H. Tobias and J. Wallaschek, "Survey of the present state of the art of piezoelectric linear motors," *Ultrasonics*, vol. 38, pp. 37-40, 2000.
- [34] V. Snitka, "Ultrasonic actuators for nanometer positioning," *Ultrasonics*, vol. 38, pp. 20-25, 2000.
- [35] [www.nanomotion.net](http://www.nanomotion.net)
- [36] M. Shafik, "Computer simulation and modelling of standing wave piezoelectric ultrasonic motor using flexural transducer, ASME 2012 International Mechanical Engineering Congress and Exposition, 2012
- [37] M. W. Lin, Abatan A. O. and Rogers C. A., "Application of commercial finite codes for the analysis of induced strain-Actuated structures," *Journal of Intelligent Material Systems and Structures*, vol. 5, pp. 869-875, 1994.
- [38] W. S. Hwang and H. C. Park, "Finite element modelling piezoelectric sensors and actuators," *AIAA J*, vol. 31, pp. 930-937, 1993.
- [39] M. Shafik and S. Fekkai, "Computer simulation and modelling of standing wave piezoelectric ultrasonic motor Using a single flexural vibration transducer," *International Journal of Applied Mechanics and Materials*, vol. 307, pp 42-52, 2013.
- [40] M. Shafik, "An investigation into the influence of ultrasonic servo drive technology in electro discharge machining industrial applications," ASME 2012 International Mechanical Engineering Congress and Exposition, 2012.
- [41] M. Shafik and H. S. Abdalla, "A micro investigation into electro discharge machining industrial applications processing parameters and surface profile using a piezoelectric ultrasonic feed drive," *ASME, J. Manuf. Sci. Eng.*, vol. 133, Aug. 2011.
- [42] J. McGeough, and H. Rasmussen, "A model for the surface texturing of steel rolls by electro discharge machining," *Proceedings: Mathematical and Physical Sciences*, vol. 436, pp. 155-164, 1992.
- [43] F. El-Menshawly, and M. S. Ahmed, "Monitoring and control of the electrical discharge texturing process for steel cold mill work roll," *Proc. of 13<sup>th</sup> North American Research Conference*, 1985, pp. 470-475.

